Toxicology Research

PAPER

Cite this: *Toxicol. Res.*, 2015, **4**, 270

Transgenerational safety of nitrogen-doped graphene quantum dots and the underlying cellular mechanism in *Caenorhabditis elegans*†

Yunli Zhao,‡[a] Qian Liu,‡[b] Shumaila Shakoor,[a] Jian Ru Gong*[b] and Dayong Wang*[a]

Nitrogen-doped graphene quantum dots (N-GQDs) are of potential use for cellular imaging. We here employed the *in vivo Caenorhabditis elegans* assay system to investigate the transgenerational behavior of N-GQDs and the underlying cellular mechanism involved. Prolonged exposure to N-GQDs did not induce lethality, lifespan reduction, or change the functions of primary and secondary targeted organs in the wild-type nematode and in nematodes with mutations of the *sod-2* or *sod-3* genes that encode Mn-SODs. Moreover, no adverse effects were detected in progeny of N-GQD-exposed wild-type and mutant nematodes. N-GQDs were only distributed in the intestine of both wild-type and mutant nematodes. No N-GQD accumulation was observed in embryos and progeny of exposed nematodes. After N-GQD exposure, the normal biological state of the intestinal barrier and defecation behavior were maintained in the wild-type and mutant nematodes. We hypothesize that the physiological states of the intestinal barrier and defecation behavior may contribute greatly to the lack of translocation of N-GQDs into secondary targeted organs and progeny of exposed nematodes. Our data provide systematic *in vivo* evidence to indicate the transgenerational safety of N-GQDs and the underlying cellular mechanism.

Received 10th September 2014,
Accepted 27th October 2014

DOI: 10.1039/c4tx00123k

www.rsc.org/toxicology

Introduction

Graphene quantum dots (GQDs) are the miniaturized versions of graphene oxide (GO) sheets, and have sizes ranging from several nanometers to tens of nanometers.[1,2] Syntheses of GQDs based on top-down or bottom-up methods,[3–8] stability of the GQDs,[9] turning of properties of the GQDs,[10] and new phenomena in energy relaxation dynamics[2] have been widely studied. Quantum confinement, which involves a crystal boundary significantly modifying the electron distribution and hence influencing properties such as bandgap size and energy relaxation dynamics,[2] has been well demonstrated in GQDs and can lead to possible practical applications for these materials.[2]

GQDs can be potentially used for photovoltaic devices,[11–15] sensors,[16–19] catalysis,[1] and DNA cleavage.[20,21] One of the most fascinating features of GQDs is their photoluminescence.[7] GQDs can be applied for high-contrast and deep-tissue bioimaging,[22–26] and labeling the cell membrane, cytoplasm, and nucleus simultaneously.[7] The recent studies have also demonstrated that GQDs have potential use in drug delivery.[21,26,27] Moreover, it has been shown that specific surface modifications of GQDs can further modify their properties and provide possibilities for more applications.[11,28] For example, GQDs functionalized with boronic acid can serve as fluorescent probes for selective and sensitive glucose determination in microdialysate.[29] Aryl-functionalized GQDs can cause enhanced photoluminescence and improved pH tolerance.[30] Polydopamine-coated GQDs could be used as long-term optical imaging agents or biocompatible drug carriers.[23]

Safety concerns regarding GQDs, however, have gradually received increasing amounts of attention as their possible industrial and medical applications have been investigated. *In vitro* toxicity assessments using various cell lines have demonstrated possible low or moderate toxicity of GQDs.[22,23,26,28,31–36] More recently, *in vivo* studies have also indicated the low toxicity of GQDs.[26,37] Nevertheless, knowledge about the *in vivo* translocation of GQDs is still very limited. Moreover, we still do not know about the possible transgenerational effects of GQDs on animals and the underlying mechanism involved.

The free-living soil nematode *Caenorhabditis elegans* (*C. elegans*) is an excellent model animal because of its short lifespan, ease of manipulation, low cost, and well-described genetic background,[38] and can serve as a useful *in vivo*

[a]*Key Laboratory of Environmental Medicine Engineering in Ministry of Education, Medical School of Southeast University, Nanjing 210009, China.*
E-mail: dayongw@seu.edu.cn
[b]*National Center for Nanoscience and Technology, Beijing 100190, China.*
E-mail: gongjr@nanoctr.cn

† Electronic supplementary information (ESI) available. See DOI: 10.1039/c4tx00123k

‡ They contributed equally to this work.

non-mammalian alternative model for toxicity assays.[39] This organism can be used for the analysis of transgenerational effects of toxicants such as heavy metals and engineered nanomaterials (ENMs) on animals.[40,41] In addition, *C. elegans* has been effectively applied for toxicological studies of different ENMs including carbon-based nanomaterials and quantum dots (QDs).[42–45] Recently, the cellular and chemical mechanisms of adverse effects of graphene oxide (GO) have also been determined in *C. elegans*.[46,47] This organism can also be used to identify those genes in animals that may be susceptible to the effects of specific ENMs.[48] Mutations of *C. elegans* genes (*sod-2* and *sod-3*) encoding manganese superoxide dismutases (Mn-SODs) have been shown to induce the susceptibility of the nematode to toxic ENMs.[49,50]

A previous study has indicated that nitrogen-doped GQDs (N-GQDs) with strong two-photon-induced fluorescence can be prepared for the use in cellular and deep-tissue imaging.[25] In the current study, we employed an *in vivo* assay system to investigate whether exposure to N-GQDs causes translocations and has adverse transgenerational effects on *C. elegans*. Our results demonstrate that several basic functions remain at normal levels in progeny of N-GQD-exposed *C. elegans*. We further determined the underlying cellular mechanism for the translocation and transgenerational behavior of N-GQDs in nematodes.

Materials and methods

Preparation and characterizations of N-GQDs

N-GQDs were prepared through a one-pot solvothermal approach using GO as a precursor as described previously.[25] The N-GQDs were characterized using various microscopic, spectroscopic, and scattering methods. Atomic force microscopy (AFM) images of N-GQDs were collected using a Dimension 3100 AFM, operating in tapping mode with a scan rate of 1.20 Hz and a resolution of 512 × 512 pixels. A 10 microliter droplet of an N-GQD aqueous solution was deposited on the top of an inclined freshly cleaved mica surface. For background subtraction, we used Nanoscope V5.31 software. The images were processed using the Flatten function to subtract the background with a flatten order of 3. A transmission electron microscopy (TEM) image was collected on an F20 S-TWIN electron microscope (Tecnai G2, FEI Company), using a 200 kV accelerating voltage. Fourier transform infrared spectroscopy (FTIR) spectra of N-GQDs were recorded on an IRAffinity-1 FTIR spectrometer. Raman spectra of N-GQDs were recorded on a Renishaw inVia plus laser Raman spectrometer with λ_{ex} = 785 nm. One-photon fluorescence spectra of N-GQDs were obtained from a Fluorolog3-21-iH320 spectrofluorometer (Jobin Yvon, France). A femtosecond Ti:Sapphire laser with high photon density was used for emission measurements. The type of laser used is an optical parametric oscillator (OPO, λ_{center} = 780 nm, 80 mHz repetition rate, 140 fs pulse width, OPAL BB, Spectra Physics) pumped by a mode-locked femtosecond Ti:Sapphire laser (Tsunami, Spectra Physics). It should be noted that a low laser power of 1 mW (average power density: 13 W cm^{-2}) was sufficient to induce strong fluorescence of the N-GQDs. Zeta potentials and the size distribution of the N-GQDs were determined by dynamic light scattering (DLS) using a Nano Zetasizer.

Strains and exposure

Nematode strains used in this study were wild-type N2, mutants of *sod-2(tm776)* and *sod-3(ok1030)*, and a transgenic strain of *oxIs12*[*Ex*(P*unc-47::GFP*)], which were maintained on nematode growth medium (NGM) plates seeded with *Escherichia coli* OP50 at 20 °C as described.[38] Gravid nematodes were washed off from NGM plates into the centrifuge tubes, and were lysed with a bleaching mixture (0.45 mol L^{-1} NaOH, 2% HOCl). Age-synchronous populations of L1-larvae were obtained as described.[51] Considering that L1-larvae are more sensitive to toxicants than are L4-larvae or adults,[52] prolonged exposures of nematodes at various stages (from L1-larvae to adult day-1) to N-GQDs were carried out in 12-well sterile tissue culture plates at 20 °C in the presence of food. To assess the possible effects of N-GQDs on progeny of exposed nematodes, eggs were obtained from animals exposed to N-GQDs by treating them with the bleaching mixture, and then transferred to a new NGM plate without addition of N-GQDs.

Lethality, reproduction, and locomotion behavior assays

For the lethality assay, a 1.0 mL aliquot of test solution was added to wells of a tissue culture plate, and each well was subsequently loaded with 50 nematodes. Following exposure, wells were observed under a dissecting microscope, where those with inactive nematodes were scored. The nematodes were judged to be dead if they did not respond to a stimulus using a small metal wire. To assay brood size, the number of offspring at each stage (beyond the egg stage) was counted. Twenty nematodes were examined per treatment. Locomotion behavior was evaluated by endpoints of head thrash and body bend. (Head thrash is defined as a change in the direction of bending at the mid body. Body bend is defined as the change in the direction of the part of the nematode corresponding to the posterior bulb of the pharynx along the *y* axis, assuming that nematode was moving along the *x* axis.) To assay locomotion behavior, the examined nematodes were washed with K medium, and transferred into a microtiter well containing 60 μL of K medium on top of agar. Twenty nematodes were examined per treatment. Three replicates were performed.

Lifespan assay

The lifespan assay was performed basically as previously described.[53] In this test, the hermaphrodites were transferred daily for the first 4 days of adulthood. Nematodes were checked every 2 days and would be scored as dead when they did not move even after repeated taps with a pick. Forty nematodes were examined per treatment. For lifespan, graphs are representative of at least three trials.

Intestinal reactive oxygen species (ROS) production

To examine the intestinal reactive oxygen species (ROS) production, nematodes were transferred to 1 μmol L^{-1} of 5′,6′-chloromethyl-2′,7′dichlorodihydro-fluorescein diacetate (CM-H_2DCFDA; Molecular Probes) in a 12-well sterile tissue culture plate to incubate for 3 hours at 20 °C. CM-H_2DCFDA can in particular detect the presence of various intracellularly produced ROS species. Nematodes were mounted on 2% agar pads for examination with a laser scanning confocal microscope (Leica, TCS SP2, Bensheim, Germany) at an excitation wavelength of 488 nm and emission filter of 510 nm. The relative fluorescence intensity of the intestine was semi-quantified, and the semi-quantified ROS was expressed as relative fluorescent units (RFU). Fifty nematodes were examined per treatment. Three replicates were performed.

Reverse transcription and quantitative real-time polymerase chain reaction (qRT-PCR)

Total RNA was extracted using RNeasy Mini Kit (Qiagen). Approximately 6000 nematodes were used for each exposure. Total nematode RNA (~1 μg) was reverse-transcribed using a cDNA Synthesis kit (Bio-Rad Laboratories). Quantitative reverse-transcription PCR was run at the optimized annealing temperature of 58 °C. The relative quantification of targeted genes in comparison to the reference *tba-1* gene encoding a tubulin protein was determined. The final results were expressed as the ratio of the relative expressions of the targeted and reference genes. The designed primers for targeted genes and reference *tba-1* gene are shown in Table S1.†

Nile Red staining

Nile Red (Molecular Probes, Eugene, OR) was dissolved in acetone to produce a 0.5 mg mL^{-1} stock solution and stored at 4 °C. Fresh stock solution was diluted in 1 × phosphate buffer saline (PBS) to 1 μg mL^{-1}, and 150 μL of the diluted solution was used for Nile Red staining. Twenty nematodes were used for each treatment. Three replicates were performed.

Defecation behavior analysis and fluorescent images of neurons controlling the defecation behavior

To assay the mean defecation cycle length, individual animals were examined for a fixed number of cycles. A cycle period was defined as the interval between the initiations of two successive posterior body-wall muscle contraction steps. Twenty replicates were performed.

Pictures of the fluorescence of AVL and DVB neurons controlling defecation behavior were taken with a Zeiss Axiocam MRm camera on a Zeiss Axioplan 2 imaging system using SlideBook software (Intelligent Imaging Innovations). Images were acquired with a Quantix cooled charge-coupled device (CCD) camera, and illumination was provided by a 175 W xenon arc lamp and GFP filter sets. The relative sizes of fluorescent puncta at the position of cell body of AVL or DVB neuron were measured as the maximum radius of the assayed fluorescent puncta and were examined in 20 nematodes. Three replicates were performed.

Statistical analysis

All data in this article were expressed as means ± standard error of the mean (S.E.M.). Graphs were generated using Microsoft Excel (Microsoft Corp., Redmond, WA). Statistical analysis was performed using SPSS 12.0 software (SPSS Inc., Chicago, USA). Differences between groups were determined using analysis of variance (ANOVA). The probability levels of 0.05 and 0.01 were considered statistically significant.

Results

Characterizations of N-GQDs

The AFM image displayed in Fig. 1A shows that the heights of N-GQDs were between 0.5 and 1 nm, implying that the graphene nanosheet monolayer is quasi-round. The TEM image further confirmed the AFM assay result (Fig. 1B). The N-GQDs dispersed in water were measured to have an average diameter of 3 nm (Fig. 1C). The UV-Vis spectrum of the N-GQDs shows an absorption band at *ca.* 230 nm, and the optical absorption edge was found to be 390 nm (Fig. 1D). The fluorescence spectrum of the N-GQDs indicates an absorption band at *ca.* 520 nm (Fig. 1E). The FTIR spectrum of the N-GQDs confirms that they were doped with nitrogen and partially reduced (Fig. 1F). The bands at 1122 cm^{-1} and 2982 cm^{-1} were assigned, respectively, to the asymmetric stretching of the C–N–C and the C–H bonds of the attached dimethylamido group (Fig. 1F). The Raman spectrum of the N-GQDs shows the D (1325 cm^{-1}) band, which is ascribed to the disordered carbon (Fig. 1G). The zeta potential of the N-GQDs used was −20 ± 1.8 mV in K medium.

Effects of N-GQD exposure on nematodes

We assessed the toxicity of N-GQDs with the aid of *C. elegans* as an *in vivo* assay system. The examined concentrations for N-GQDs were 0.1–100 mg L^{-1}. Prolonged exposure of L1-larvae to adult day-1 to these concentrations of N-GQDs was not lethal (data not shown) and did not in any obvious manner affect the average lifespan of the nematodes (Fig. 2A).

Although toxic ENMs could adversely influence the functions of both primary targeted organs such as intestines and secondary targeted organs such as neurons and reproductive organs in *C. elegans*,[54] prolonged exposure to N-GQDs (0.1–100 mg L^{-1}) in our experiments did not significantly reduce the brood size (Fig. 2B) and did not decrease the locomotion behavior as reflected by endpoints of body bends and head thrashes (Fig. 2C), implying the relatively normal physiological functions of their neurons and reproductive organs in our case. Moreover, we did not observe a noticeable induction of intestinal ROS production in nematodes exposed to N-GQDs (0.1–100 mg L^{-1}) (Fig. 2D). Therefore, using our assay system, we did not detect obvious adverse effects of N-GQDs on *C. elegans*.

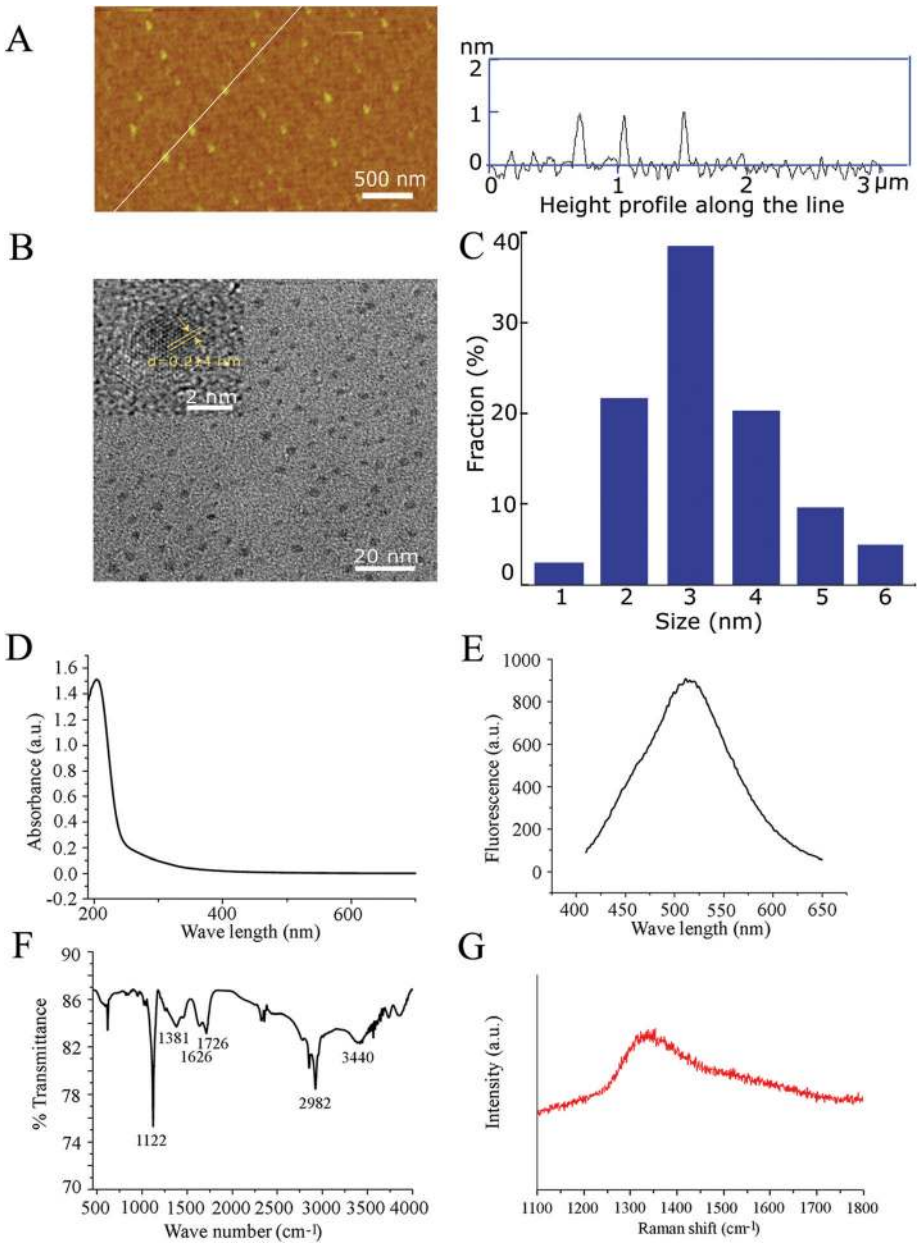

Fig. 1 Characterizations of N-GQDs. (A) AFM image of N-GQDs and the height profile along the white line in the AFM image. (B) TEM image of N-GQDs. (C) Distribution of the diameters of N-GQDs. (D) UV-Vis absorption spectrum of the N-GQDs. (E) Fluorescence spectrum of N-GQDs under 800 nm excitation. (F) FTIR spectrum of N-GQDs. (G) Raman spectrum of N-GQDs.

Effects of N-GQD exposure on progeny of exposed nematodes

The toxicity of some toxicants can be transferred and even be amplified in the progeny of exposed nematodes.[40,41] To exclude this possibility, we investigated the effects of N-GQD exposure on progeny (F1) of exposed nematodes (P0). After prolonged exposure, the eggs of N-GQD-exposed nematodes were transferred to new NGM plates without addition of N-GQDs. In the F1 progeny of the nematodes exposed to N-GQDs (0.1–100 mg L^{-1}), we observed neither induction of lethality (data not shown) nor any noticeable reduction of lifespan (Fig. 3A) nor significant reduction of brood size (Fig. 3B) nor decrease in locomotion behavior (Fig. 3C) nor significant induction of intestinal ROS production (Fig. 3D). These data suggest that the normal physiological functions of primary and secondary targeted organs can be sustained in F1 progeny of N-GQD-exposed nematodes.

Effects of N-GQD exposure on nematodes with mutations of genes encoding Mn-SODs

In *C. elegans*, mutations of either the *sod-2* or *sod-3* genes do usually cause susceptibility to toxicants including toxic ENMs.[49,50] We therefore next asked whether prolonged exposure to N-GQDs

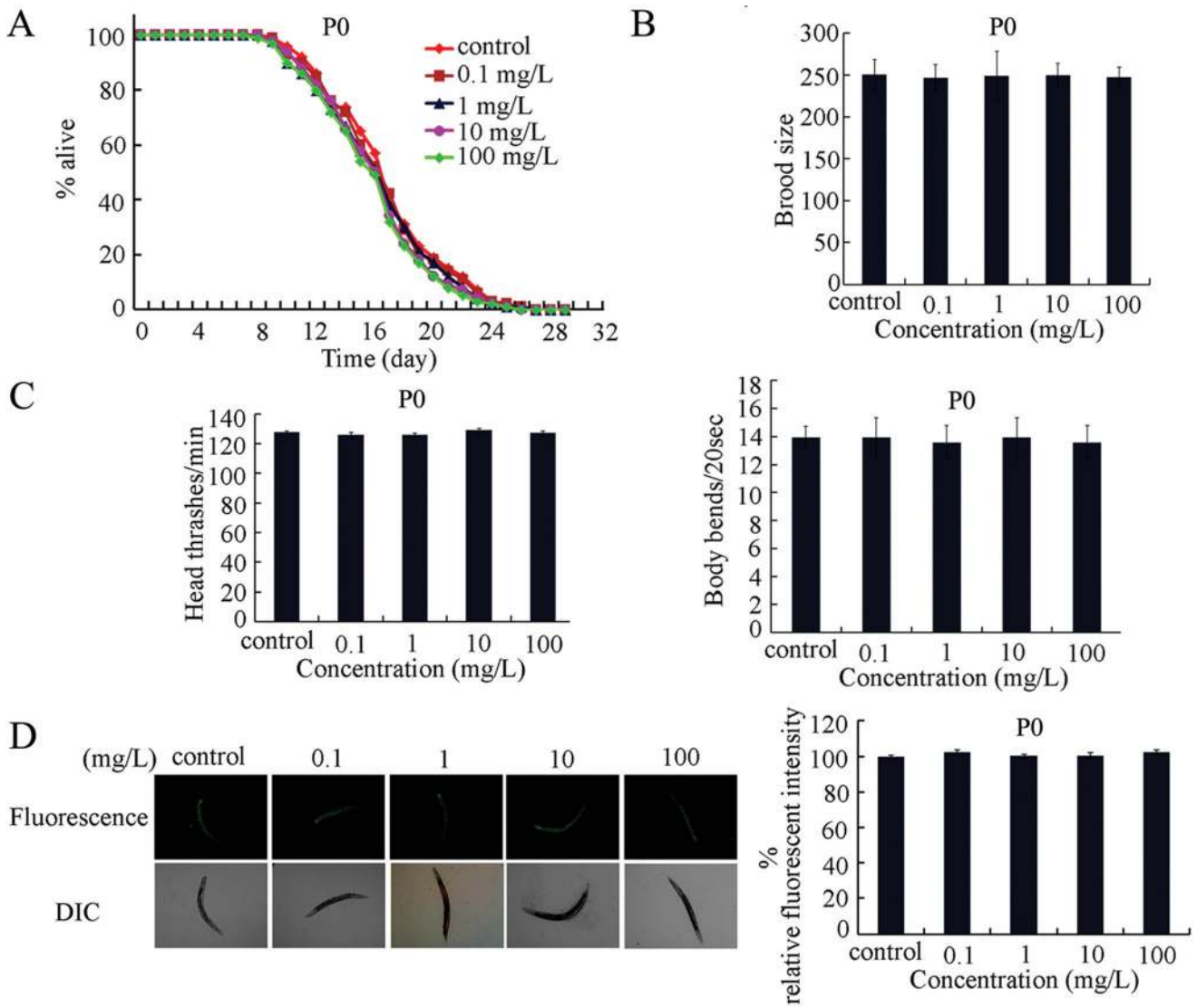

Fig. 2 Effects of N-GQD exposure on animals. (A) Effect of N-GQDs on lifespan of nematodes. (B) Effect of N-GQDs on brood size of nematodes. (C) Effect of N-GQDs on locomotion behavior in nematodes. (D) Effect of N-GQDs on induction of intestinal ROS production. Prolonged exposure was performed from L1-larvae to adult day-1. Bars represent means ± standard error of the mean (S.E.M.).

at the examined concentrations would be safe for nematodes with mutations to these genes. Prolonged exposure to N-GQDs (100 mg L^{-1}) neither induced lethality (data not shown) nor caused an obvious reduction of lifespan (Fig. 4A) nor significantly decreased brood size (Fig. 4B) nor significantly decreased locomotion behavior (Fig. 4C) nor induced significant induction of intestinal ROS production (Fig. 4D) in both the *sod-2* and *sod-3* mutant nematodes. Therefore, the physiological functions of both primary and secondary targeted organs can also be sustained at the normal state in nematodes with mutations of genes encoding Mn-SODs. Even more interestingly, we also did not detect any obvious adverse effects of N-GQDs on physiological functions of both primary and secondary targeted organs in F1 progeny of exposed *sod-2* and *sod-3* mutant nematodes (data not shown).

Effects of N-GQD exposure on expression patterns of genes required for oxidative stress in exposed nematodes and their progeny

In *C. elegans*, the oxidative stress is under the control of a series of genes.[50] Among these genes, the *sod-1* gene encodes a copper/zinc SOD, the *sod-2* and *sod-3* genes encode Mn-SODs, the *sod-4* and *sod-5* genes encode extracellular copper/zinc SODs, the *gas-1* gene encodes a subunit of mitochondrial complex I, the *mev-1* gene encodes a subunit of mitochondrial complex II, the *isp-1* gene encodes a subunit of mitochondrial complex III, the *clk-1* gene encodes a demethoxyubiquinone hydroxylase that is necessary for the synthesis of ubiquinone, and the *ctl-1*, *ctl-2*, and *ctl-3* genes encode catalases. We observed that prolonged exposure to N-GQDs (100 mg L^{-1}) did not significantly affect the expression patterns of the SOD-encoding genes (*sod-1*, *sod-2*, *sod-3*, *sod-4*, and *sod-5*) (Fig. S1†).

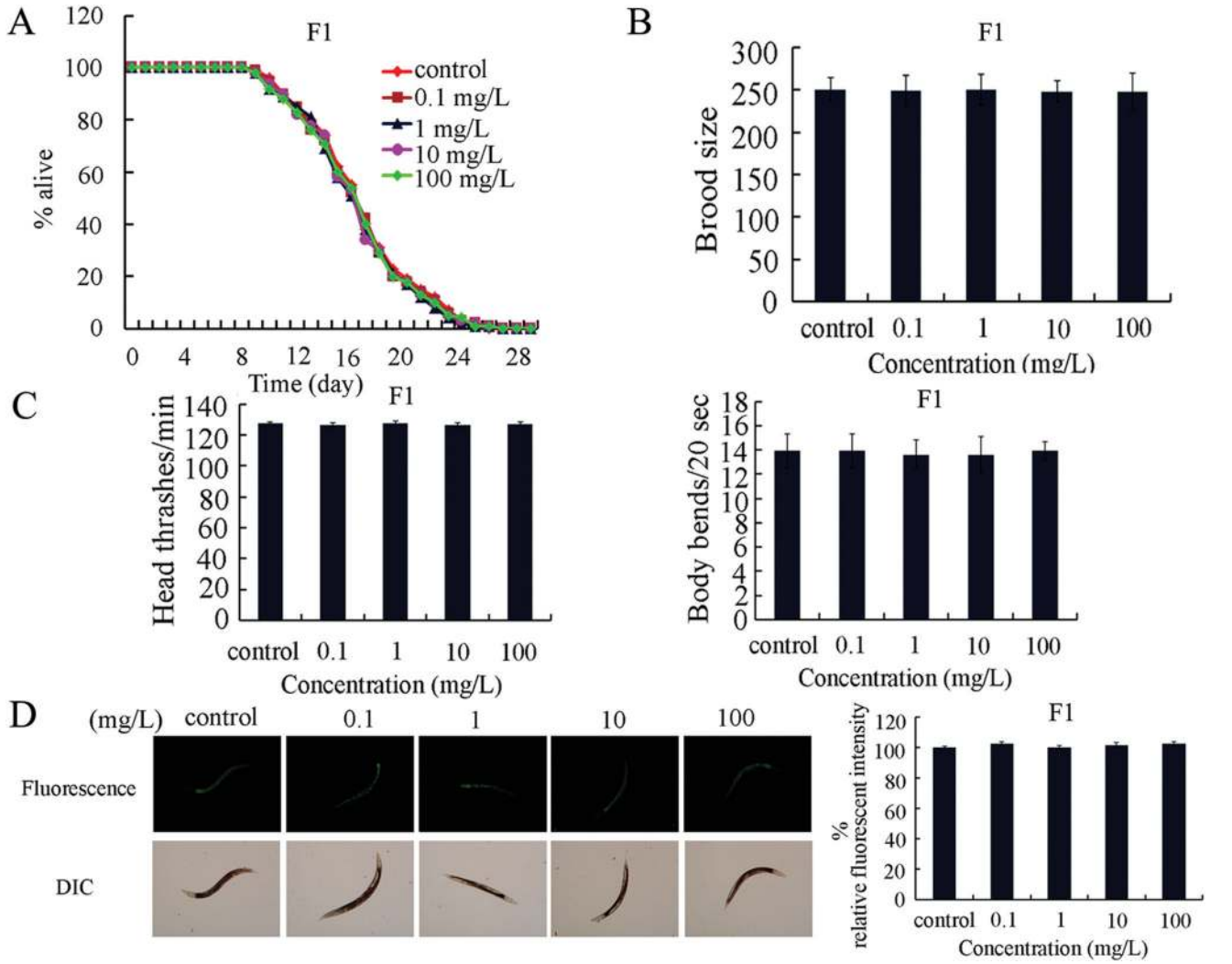

Fig. 3 Phenotypic analysis in progeny of nematodes exposed to N-GQDs. (A) Lifespan in progeny of nematodes exposed to N-GQDs. (B) Brood size in progeny of nematodes exposed to N-GQDs. (C) Locomotion behavior in progeny of nematodes exposed to N-GQDs. (D) Intestinal ROS production in progeny of nematodes exposed to N-GQDs. Prolonged exposure was performed from L1-larvae to adult day-1. Bars represent means ± standard error of the mean (S.E.M.).

We also did not detect a noticeable change in the expression patterns of the *sod-1*, *sod-2*, *sod-3*, *sod-4*, and *sod-5* genes in the F1 progeny of nematodes exposed to N-GQDs (100 mg L^{-1}) (Fig. S1†). Similarly, we neither observed an obvious alteration of the expression patterns of *mev-1*, *isp-1*, *gas-1*, *clk-1*, *ctl-1*, *ctl-2*, and *ctl-3* genes in nematodes exposed to N-GQDs (100 mg L^{-1}) nor in their F1 progeny (data not shown). These results further support the relative safety of the prepared N-GQDs for nematodes.

Distribution and translocation of N-GQDs in nematodes

Bioavailability is very important for specific ENMs to actually be toxic for nematodes.[54] To determine the cellular basis for the observed lack of toxicity of N-GQDs, we further investigated the distribution and translocation of N-GQDs in nematodes. After prolonged exposure, we found that N-GQDs were mainly distributed in the intestines of wild-type nematodes (Fig. 5A) as well as of *sod-2* and *sod-3* mutant nematodes (Fig. 5A). We did not observe the translocation of N-GQDs into the secondary targeted organs such as neurons and reproductive organs through the biological barrier of the intestine in both wild-type and mutant (*sod-2* or *sod-3*) nematodes (Fig. 5A). We also did not detect the green fluorescence signals of N-GQDs in F1 progeny of exposed wild-type nematodes (Fig. 5A), and we did not detect these N-GQD signals in embryos of the exposed wild-type, *sod-2*, and *sod-3* mutant nematodes (Fig. 5B). These results suggest that N-GQDs can only be distributed in the intestine, and do not cross the biological barrier of the intestine to be translocated into the secondary targeted organs in nematodes.

N-GQD exposure does not obviously alter the intestinal permeability

Intestinal permeability is one of the crucial factors influencing the distribution and translocation of ENMs in nematodes.[47]

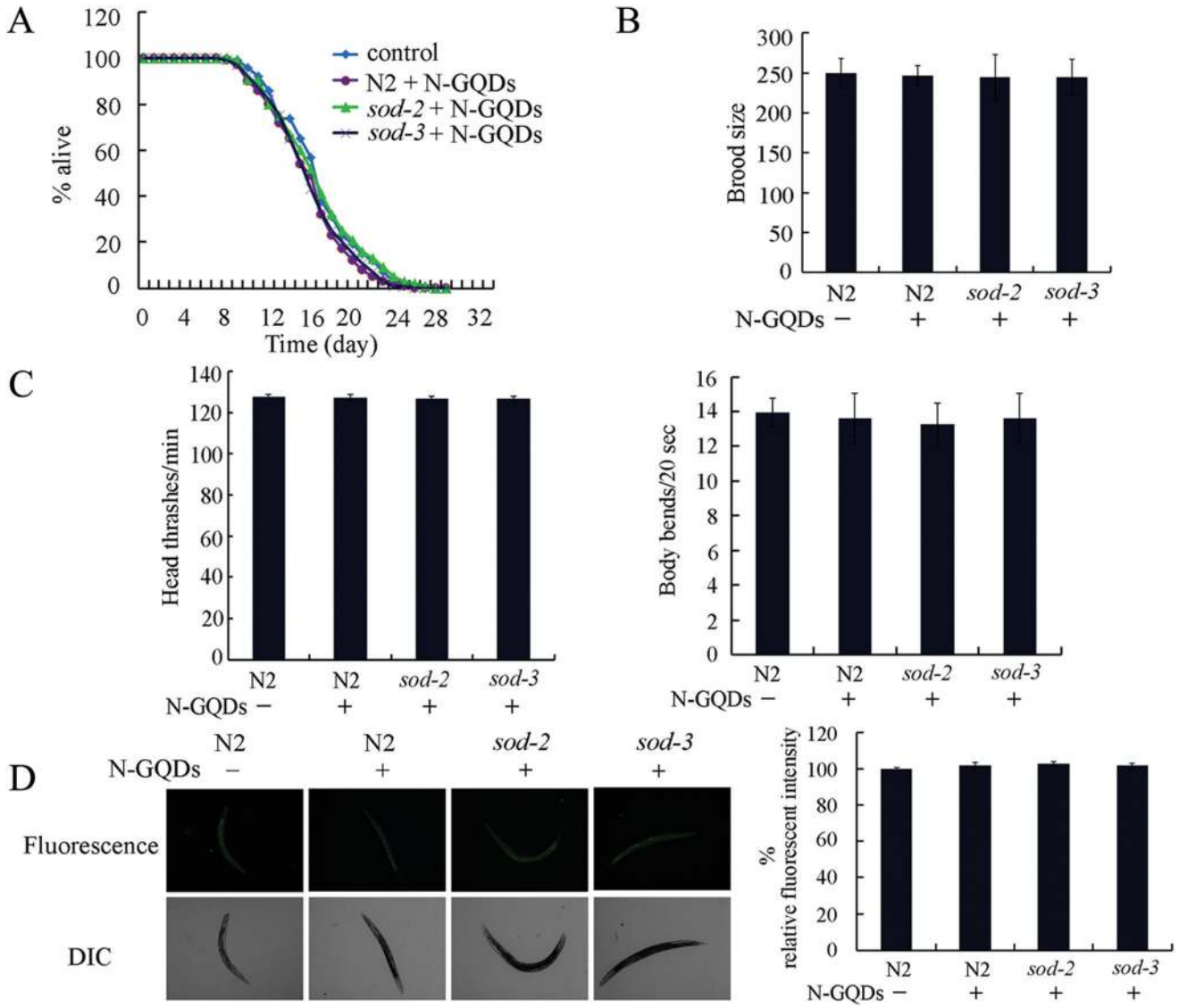

Fig. 4 Effects of N-GQD exposure on *sod-2* and *sod-3* mutant animals. (A) Effects of N-GQDs on lifespans of *sod-2* and *sod-3* mutant nematodes. (B) Effects of N-GQDs on brood sizes of *sod-2* and *sod-3* mutant nematodes. (C) Effects of N-GQDs on locomotion behavior in *sod-2* and *sod-3* mutant nematodes. (D) Effects of N-GQDs on induction of intestinal ROS production in *sod-2* and *sod-3* mutant nematodes. Prolonged exposure to 100 mg L^{-1} of N-GQDs was performed from L1-larvae to adult day-1. Bars represent means ± standard error of the mean (S.E.M.).

Considering the important role of primary targeted organs in regulating the translocation and distribution of ENMs, we investigated the permeability of these organs in N-GQD-exposed nematodes. We used the lipophilic fluorescent dye Nile Red to stain the N-GQD-exposed nematodes. Prolonged exposure to N-GQDs (100 mg L^{-1}) did not obviously affect the relative fluorescence intensity of Nile Red in intestines of wild-type, *sod-2*, or *sod-3* mutant nematodes compared with that of the control (Fig. 6). Similarly, the relative fluorescence intensity of Nile Red in the intestines of F1 progeny of N-GQD-exposed nematodes was similar to that of the control (Fig. 6). These data imply that prolonged exposure to N-GQDs may have no noticeable effect on the permeability of the intestinal barrier in nematodes. That is, intestinal barriers of nematodes can effectively maintain their normal state of permeability when exposed to N-GQDs.

N-GQD exposure does not influence defecation behavior and structure of neurons regulating defecation behavior

Defecation behavior is another crucial factor influencing the distribution and translocation of ENMs in nematodes.[47] Besides maintaining normal intestinal permeability, the N-GQD-exposed nematodes would also need to show normal defecation behavior in order for N-GQDs to be considered safe. For this purpose, and to examine the possible mechanism explaining the safety of N-GQD exposure, we next investigated the effects of N-GQD exposure on defecation behavior. Prolonged exposure to N-GQDs (100 mg L^{-1}) yielded similar defecation behavior in wild-type, *sod-2*, and *sod-3* mutant nematodes as in the control (Fig. 7A). The mean defecation cycle time in F1 progeny of nematodes exposed to N-GQDs (100 mg L^{-1}) was also similar to that of the control (Fig. 7A).

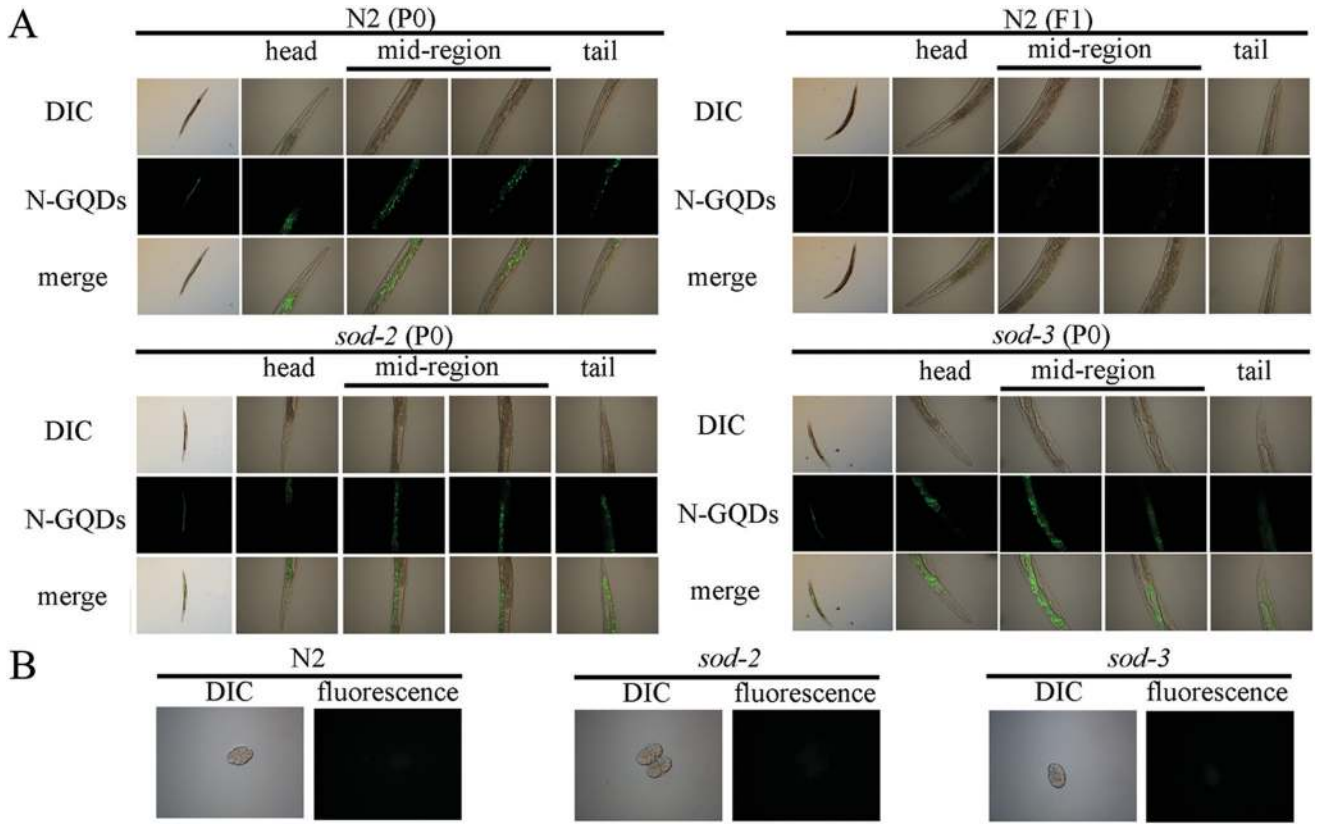

Fig. 5 Distribution and translocation of N-GQDs in nematodes. (A) Distribution of N-GQDs in exposed nematodes and their progeny. (B) Distribution of N-GQDs in embryos of exposed wild-type, *sod-2*, and *sod-3* mutant nematodes. Prolonged exposure to 100 mg L^{-1} of N-GQDs was performed from L1-larvae to adult day-1.

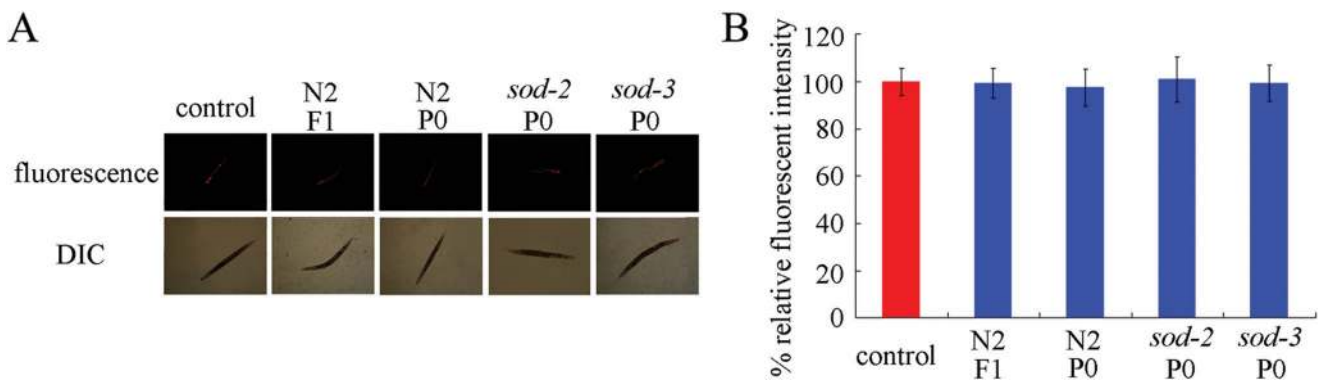

Fig. 6 Intestinal permeability in nematodes exposed to N-GQDs. (A) Nile Red staining of nematodes. (B) Comparison of intestinal fluorescence intensity of Nile Red. Prolonged exposure to 100 mg L^{-1} of N-GQDs was performed from L1-larvae to adult day-1. Bars represent means ± standard error of the mean (S.E.M.).

In *C. elegans*, AVL and DVB neurons are involved in the regulation of defecation behavior.[55] Again, we used a transgenic strain of *oxIs12*, in which both AVL and DVB neurons in GABAergic nervous system were labeled with green fluorescent protein, to investigate any possible structural alteration of these neurons in N-GQD-exposed nematodes. We found that the structures of both the AVL and DVB neurons were not obviously altered in wild-type, *sod-2*, and *sod-3* mutant nematodes exposed to N-GQDs (100 mg L^{-1}) compared with the control (Fig. 7B and C). In addition, the structures of both AVL and DVB neurons in F1 progeny of nematodes exposed to N-GQDs (100 mg L^{-1}) were similar to those of the controls (Fig. 7B and C). Therefore, besides the permeable state of the intestinal barrier, the defecation state also appears to serve as an important indicator of the lack of toxicity of N-GQDs in nematodes.

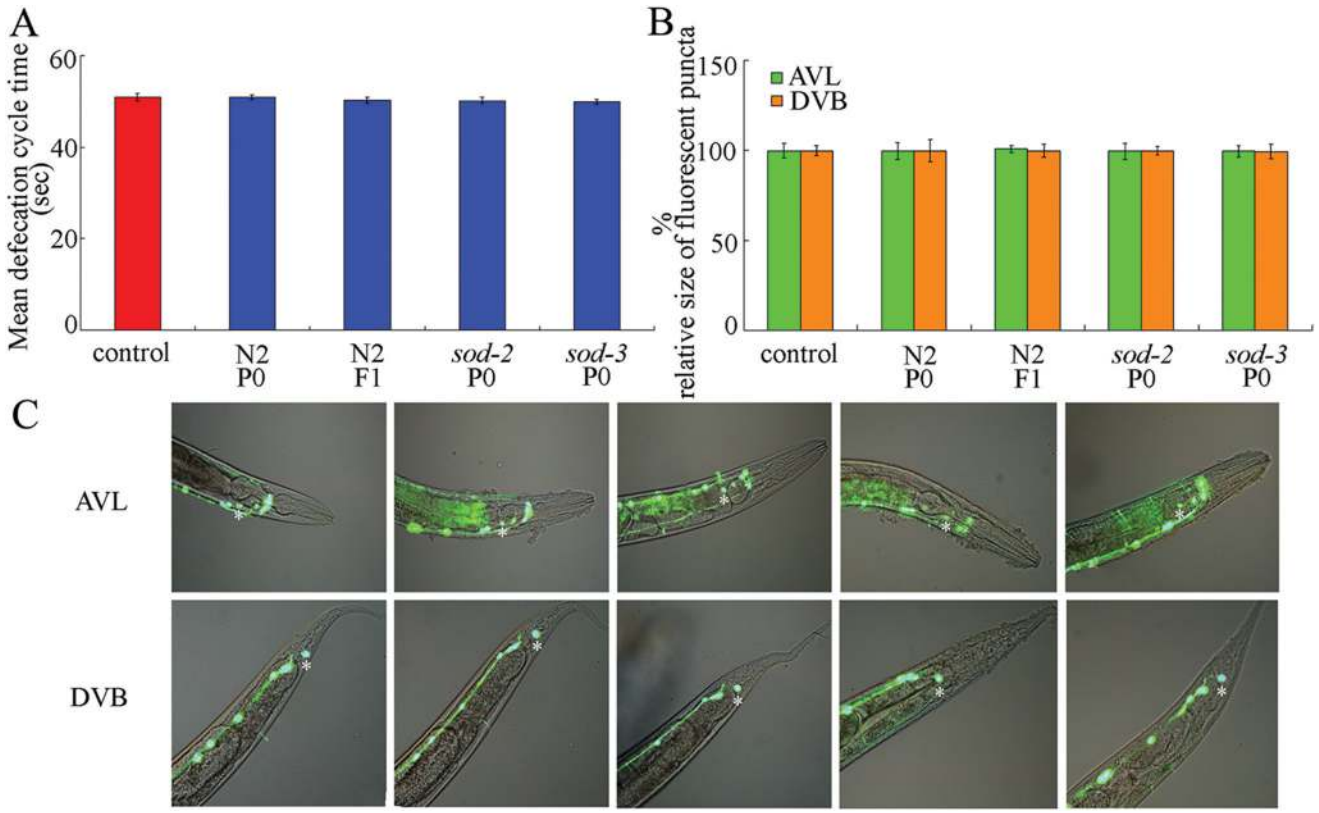

Fig. 7 Maintenance of normal defecation behavior and structure of neurons controlling defecation in N-GQDs exposed nematodes. (A) Defecation behavior in N-GQDs exposed nematodes. (B) Relative sizes of AVL and DVB neurons in N-GQD-exposed nematodes. (C) Pictures showing the AVL and DVB neurons in N-GQD-exposed nematodes. Prolonged exposure to 100 mg L^{-1} of N-GQDs was performed from L1-larvae to adult day-1. In each picture, the asterisk indicates the position of the AVL or DVB neuron. Bars represent means ± standard error of the mean (S.E.M.).

Moreover, we directly observed the metabolism of N-GQDs in nematodes. To observe such dynamic metabolism, we transferred the exposed nematodes to the normal NGM plants without addition of N-GQDs. At least three stages of the metabolism of N-GQDs were observed in the nematodes. Initially, after feeding, the N-GQDs were strongly distributed in the pharynx, intestine, and tail regions where the GQDs would be excreted out of the body (Fig. S2†). At the second stage, we found that the distribution of N-GQDs in the pharynx was gradually decreased, and N-GQDs were mainly distributed in the intestine and tail region (Fig. S2†). At the third stage, no strong N-GQD fluorescent signals were observed in the nematodes (Fig. S2†).

Discussion

The previous study has demonstrated that the high two-photon absorption, large imaging depth and extraordinary photostability render N-GQDs a potential alternative probe for efficient two-photon imaging in both biological and medical applications.[25] The *in vitro* cytotoxicity assay suggested the low toxicity of N-GQDs at concentrations of 5–400 mg L^{-1}.[25] Previous studies have also demonstrated that the GQDs at concentrations of not more than 100 mg L^{-1} are relatively safe for different examined cancer cell lines such as the breast cancer MCF-7 cell.[26,36,37] In the present study, we further provide evidence to indicate that N-GQDs are relatively safe, in an *in vivo* assay system using *C. elegans*. Prolonged exposure to N-GQDs (0.1–100 mg L^{-1}) from L1-larvae to adult neither induced lethality nor lifespan reduction nor did it cause obvious alterations in the functions of both primary and secondary targeted organs in wild-type nematodes (Fig. 2). Exposure to 5–10 mg kg^{-1} also did not cause obvious toxic effects on mice.[37] Therefore, both the *in vitro* and *in vivo* results indicate that it is relatively safe to use N-GQDs for industrial and medical applications.

In *C. elegans*, some toxicants may not only adversely affect the exposed parental animals but also influence their progeny.[40,41] The adverse effects of some toxicants on progeny may sometimes be more severe than those on their parental animals.[40] To exclude the possibility that adverse effects were transferred from exposed nematodes to their progeny and that any such adverse effects may have become severe in the progeny nematodes, we examined the transgenerational effects of N-GQDs on wild-type nematodes. Interestingly, we detected no adverse effects in the F1 progeny of N-GQD-exposed nematodes (Fig. 3). These results imply at least two possibilities. One possibility is that N-GQDs cannot be translocated into the gonads and embryos. Another possibility is that the possible

adverse effects are very weak, and cannot be strengthened in F1 progeny of N-GQD-exposed nematodes.

Previous studies have demonstrated that specific genetic mutations, such as *sod-2* and *sod-3* mutations, could cause nematodes to become susceptible to toxic effects of ENMs.[48–50] In the present study, however, we did not detect adverse effects in N-GQD-exposed *sod-2* or *sod-3* mutant nematodes (Fig. 4) and their F1 progeny. In addition, N-GQDs did not alter the expression patterns of genes required for oxidative stress in nematodes (Fig. S1†). Although we cannot exclude that nematodes with mutations to other genes may become susceptible to N-GQD exposure, our data here at least suggest that N-GQDs may not be able to induce susceptibility in nematodes with mutations of genes required for oxidative stress.

With regards to the distribution and translocation of N-GQDs in nematodes, we found that the N-GQDs were only distributed in the intestines of wild-type and mutant nematodes (Fig. 5). Moreover, no accumulation of N-GQDs was detected in embryos and F1 progeny of exposed nematodes (Fig. 5). Our results indicate that, after prolonged exposure, N-GQDs could not be translocated into secondary targeted organs through the biological barrier of the intestine, and N-GQDs are instead excreted directly out of the body of nematodes. These data are in agreement with our observations on the effects of N-GQDs on wild-type and the examined mutant nematodes and their F1 progeny.

The analysis of the biological states of the intestinal barrier and defecation behavior further supports the possible cellular mechanism for the lack of toxicity of N-GQDs in nematodes. The Nile Red staining results suggest the normal biological state of the intestinal barrier in wild-type and the examined mutant nematodes (Fig. 6), which implies a possible shielding effect of the intestinal barrier on exogenous N-GQDs nanoparticles in nematodes. The normal defecation behavior and structure of AVL and DVB neurons in wild-type and the examined mutant nematodes (Fig. 7) suggest the potentially effective excretion of N-GQDs out of the body of nematodes. We also provide evidence to indicate the possible normal biological states of the intestinal barrier and defecation behavior in F1 progeny of N-GQD-exposed nematodes (Fig. 6 and 7), which further confirms the normal functions of both primary and secondary targeted organs and no accumulation of N-GQDs in F1 progeny of exposed nematodes.

Conclusions

Our *in vivo* results suggest that N-GQDs are not toxic to wild-type and the examined mutant nematodes. More importantly, we found that N-GQDs would not be translocated into the secondary targeted organs and embryos of nematodes after feeding, and no adverse effects were detected in F1 progeny of N-GQD-exposed wild-type or examined mutant nematodes. We raise a hypothesis here that the normal physiological states of the intestinal barrier and defecation behavior may contribute greatly to the lack of translocation of N-GQDs into the secondary targeted organs and the progeny of exposed nematodes. While research on GQDs is still at the early stages and there remains much to investigate with regards to GQDs, our study at least provides an important foundation for future industrial and medical applications as well as evaluations of the safety of N-GQD release into the environment.

Funding

This work was supported by the grants from National Basic Research Program of China (no. 2011CB33404), National Natural Science Foundation of China (no. 81172698), Jiangsu Province Ordinary University Graduate Research and Innovation Program (no. CXZZ13_0136), and Fundamental Research Funds for the Central Universities.

Conflict of interest

None of the authors have any conflicting interests.

References

1 J. Shen, Y. Zhu, X. Yang and C. Li, *Chem. Commun.*, 2012, **48**, 3686–3699.
2 X. Yan, B. Li and L. Li, *Acc. Chem. Res.*, 2013, **46**, 2254–2262.
3 X. Yan, X. Cui and L. Li, *J. Am. Chem. Soc.*, 2010, **132**, 5944–5945.
4 D. Pan, J. Zhang, Z. Li and M. Wu, *Adv. Mater.*, 2010, **22**, 734–738.
5 R. Liu, D. Wu, X. Feng and K. Mullen, *J. Am. Chem. Soc.*, 2011, **133**, 15221–15223.
6 A. Barreiro, H. S. van der Zant and L. M. K. Vandersypen, *Nano Lett.*, 2012, **12**, 6096–6100.
7 L. Li, G. Wu, G. Yang, J. Peng, J. Zhao and J. Zhu, *Nanoscale*, 2013, **5**, 4015–4039.
8 F. Liu, M. Jang, H. D. Ha, J. Kim, Y. Cho and T. S. Seo, *Adv. Mater.*, 2013, **25**, 3657–3662.
9 X. Yan, Q. Li and L. Li, *J. Am. Chem. Soc.*, 2012, **134**, 16095–16098.
10 K. A. Ritter and J. W. Lyding, *Nat. Mater.*, 2009, **8**, 235–242.
11 H. Tetsuka, R. Asahi, A. Nagoya, K. Okamoto, I. Tajima, R. Ohta and A. Okamoto, *Adv. Mater.*, 2012, **24**, 5333–5338.
12 V. Gupta, N. Chaudhary, R. Srivastava, G. D. Sharma, R. Bhardwaj and S. Chand, *J. Am. Chem. Soc.*, 2011, **133**, 9960–9963.
13 I. P. Hamilton, B. Li, X. Yan and L. Li, *Nano Lett.*, 2011, **11**, 1524–1529.
14 Y. Li, Y. Hu, Y. Zhao, G. Shi, L. Deng, Y. Hou and L. Qu, *Adv. Mater.*, 2011, **23**, 776–780.
15 J. K. Kim, M. J. Park, S. J. Kim, D. H. Wang, S. P. Cho, S. Bae, J. H. Park and B. H. Hong, *ACS Nano*, 2013, **7**, 7207–7212.

16 W. Tu, W. Wang, J. Lei, S. Deng and H. Ju, *Chem. Commun.*, 2012, **48**, 6535–6537.
17 T. S. Sreeprasad, A. A. Rodriguez, J. Colston, A. Graham, E. Shishkin, V. Pallem and V. Berry, *Nano Lett.*, 2013, **13**, 1757–1763.
18 X. Ran, H. Sun, F. Pu, J. Ren and X. Qu, *Chem. Commun.*, 2013, **49**, 1079–1081.
19 Y. Zhang, C. Wu, X. Zhou, X. Wu, Y. Yang, H. Wu, S. Guo and J. Zhang, *Nanoscale*, 2013, **5**, 1816–1819.
20 X. Zhou, Y. Zhang, C. Wang, X. Wu, Y. Yang, B. Zheng, H. Wu, S. Guo and J. Zhang, *ACS Nano*, 2012, **6**, 6592–6599.
21 C. Wang, C. Wu, X. Zhou, T. Han, X. Xin, J. Wu, J. Zhang and S. Guo, *Sci. Rep.*, 2013, **3**, 2852.
22 S. Zhu, J. Zhang, C. Qiao, S. Tang, Y. Li, W. Yuan, B. Li, L. Tian, F. Liu, R. Hu, H. Gao, H. Wei, H. Zhang, H. Sun and B. Yang, *Chem. Commun.*, 2011, **47**, 6858–6860.
23 M. Nurunnabi, Z. Khatun, M. Nafiujjaman, D. Lee and Y. Lee, *ACS Appl. Mater. Interfaces*, 2013, **5**, 8246–8253.
24 H. Sun, L. Wu, N. Gao, J. Ren and X. Qu, *ACS Appl. Mater. Interfaces*, 2013, **5**, 1174–1179.
25 Q. Liu, B. Guo, Z. Rao, B. Zhang and J. Gong, *Nano Lett.*, 2013, **13**, 2436–2441.
26 Abdullah-Al-Nahain, J. Lee, I. In, H. Lee, K. D. Lee, J. H. Jeong and S. Y. Park, *Mol. Pharm.*, 2013, **10**, 3736–3744.
27 Z. Wang, J. Xia, C. Zhou, B. Via, Y. Xia, F. Zhang, Y. Li, L. Xia and J. Tang, *Colloids Surf., B*, 2013, **112**, 192–196.
28 F. Jiang, D. Chen, R. Li, Y. Wang, G. Zhang, S. Li, J. Zheng, N. Huang, Y. Gu, C. Wang and C. Shu, *Nanoscale*, 2013, **5**, 1137–1142.
29 Z. Qu, X. Zhou, L. Gu, R. Lan, D. Sun, D. Yu and G. Shi, *Chem. Commun.*, 2013, **49**, 9830–9832.
30 P. Luo, Z. Ji, C. Li and G. Shi, *Nanoscale*, 2013, **5**, 7361–7367.
31 Y. Dong, C. Chen, X. Zheng, L. Gao, Z. Cui, H. Yang, C. Guo, Y. Chi and C. M. Li, *J. Mater. Chem.*, 2012, **22**, 8764–8766.
32 J. Peng, W. Gao, B. K. Gupta, Z. Liu, R. Romero-Aburto, L. Ge, L. Song, L. B. Alemany, X. Zhan, G. Gao, S. A. Vithayathil, B. A. Kaipparettu, A. A. Marti, T. Hayashi, J. J. Zhu and P. M. Ajayan, *Nano Lett.*, 2012, **12**, 844–849.
33 M. Zhang, L. Bai, W. Shang, W. Xie, H. Ma, Y. Fu, D. Fang, H. Sun, L. Fan, M. Han, C. Liu and S. Yang, *J. Mater. Chem.*, 2012, **22**, 7461–7467.
34 S. Zhu, S. Zhang, C. Tang, L. Qiao, L. Wang, H. Wang, X. Liu, B. Li, Y. Li, W. Yu, X. Wang, H. Sun and B. Yang, *Adv. Funct. Mater.*, 2012, **22**, 4732–4740.
35 C. Hu, Y. Liu, Y. Yang, J. Cui, Z. Huang, Y. Wang, L. Yang, H. Wang, Y. Xiao and J. Rong, *J. Mater. Chem. B*, 2013, **1**, 39–42.
36 C. Wu, C. Wang, T. Han, X. Zhou, S. Guo and J. Zhang, *Adv. Healthcare Mater.*, 2013, **2**, 1613–1619.
37 M. Nurunnabi, Z. Khatun, K. M. Huh, S. Y. Park, D. Y. Lee, K. J. Cho and Y. Lee, *ACS Nano*, 2013, **8**, 6858–6967.
38 S. Brenner, *Genetics*, 1974, **77**, 71–94.
39 M. C. K. Leung, P. L. Williams, A. Benedetto, C. Au, K. J. Helmcke, M. Aschner and J. N. Meyer, *Toxicol. Sci.*, 2008, **106**, 5–28.
40 D.-Y. Wang and Y. Wang, *Environ. Pollut.*, 2008, **151**, 585–592.
41 E. Q. Contreras, M. Cho, H. Zhu, H. L. Puppala, G. Escalera, W. Zhong and V. L. Colvin, *Environ. Sci. Technol.*, 2013, **47**, 1148–1154.
42 N. Mohan, C. Chen, H. Hsieh, Y. Wu and H. Chang, *Nano Lett.*, 2010, **10**, 3692–3699.
43 Y. Qu, W. Li, Y. Zhou, X. Liu, L. Zhang, L. Wang, Y. Li, A. Iida, Z. Tang, Y. Zhao, Z. Chai and C. Chen, *Nano Lett.*, 2011, **11**, 3174–3183.
44 E. Zanni, G. De Bellis, M. P. Bracciale, A. Broggi, M. L. Santarelli, M. S. Sarto, C. Palleschi and D. Uccelletti, *Nano Lett.*, 2012, **12**, 2740–2744.
45 P. Chen, K. Hsiao and C. Chou, *Biomaterials*, 2013, **34**, 5661–5669.
46 W. Zhang, C. Wang, Z. Li, Z. Lu, Y. Li, J. Yin, Y. Zhou, X. Gao, Y. Fang, G. Nie and Y. Zhao, *Adv. Mater.*, 2012, **24**, 5391–5397.
47 Q.-L. Wu, L. Yin, X. Li, M. Tang, T. Zhang and D.-Y. Wang, *Nanoscale*, 2013, **5**, 9934–9943.
48 J. Roh, S. J. Sim, J. Yi, K. Park, K. H. Chung, D. Ryu and J. Choi, *Environ. Sci. Technol.*, 2009, **43**, 3933–3940.
49 Q. Rui, Y.-L. Zhao, Q.-L. Wu, M. Tang and D.-Y. Wang, *Chemosphere*, 2013, **93**, 2289–2296.
50 Y.-X. Li, W. Wang, Q.-L. Wu, Y.-P. Li, M. Tang, B.-P. Ye and D.-Y. Wang, *PLoS One*, 2012, **7**, e44688.
51 S. Donkin and P. L. Williams, *Environ. Toxicol. Chem.*, 1995, **14**, 2139–2147.
52 X.-J. Xing and D.-Y. Wang, *Bull. Environ. Contam. Toxicol.*, 2009, **83**, 530–536.
53 K.-W. He, L.-L. Shen, W.-W. Zhou and D.-Y. Wang, *Neurosci. Bull.*, 2009, **25**, 335–342.
54 Y.-L. Zhao, Q.-L. Wu, Y.-P. Li and D.-Y. Wang, *RSC Adv.*, 2013, **3**, 5741–5757.
55 Y.-L. Zhao, Q.-L. Wu, M. Tang and D.-Y. Wang, *Nanomedicine: Nanotechnol. Biol. Med.*, 2014, **10**, 89–98.

